Biradical Thermochemistry from Collision-Induced Dissociation Threshold Energy Measurements. Absolute Heats of Formation of *ortho*-, *meta*-, and *para*-Benzyne

Paul G. Wenthold and Robert R. Squires*

Contribution from the Department of Chemistry, Purdue University, West Lafayette, Indiana 47907

Received September 27, 1993. Revised Manuscript Received April 22, 1994•

Abstract: The absolute heats of formation of 1,2-, 1,3-, and 1,4-dehydrobenzene (*ortho*-, *meta*-, and *para*-benzyne) have been determined from measurements of the threshold energies for collision-induced dissociation (CID) of *ortho*-, *meta*-, and *para*-chlorophenyl anions in a flowing afterglow–triple quadrupole apparatus. The 298 K heats of formation for *ortho*-, *meta*-, and *para*-benzyne derived in this manner are 106.6 ± 3.0, 122.0 ± 3.1, and 137.3 ± 3.3 kcal/mol, respectively. The values for *meta*- and *para*-benzyne are higher than those reported previously (Wenthold, P. G.; Paulino, J. A.; Squires, R. R., *J. Am. Chem. Soc.* **1991**, *113*, 7414) but are in excellent agreement with recently reported MCSCF and CI calculations. Several control experiments are described which demonstrate that the earlier results for *meta*- and *para*-benzyne suffered from an acid-catalyzed isomerization of the reactant chlorophenyl anions in the flowing afterglow prior to CID threshold analysis. It is shown that CID threshold measurements with chlorophenyl-d_4 anions are necessary in order to obtain the correct dissociation energies for the isomerically pure species. The gas-phase acidities of the *meta* and *para* positions of chlorobenzene were determined at 298 K using the silane cleavage method to be 391.1 ± 2.0 and 393.9 ± 2.0 kcal/mol, respectively. The heats of formation for the benzynes determined in this study are used to derive the gas-phase acidity of the 2-position of *meta*-benzyne (365 ± 3 kcal/mol) and the *ortho*, *meta*, and *para* C–H bond strengths in phenyl radical (79.9 ± 3.1, 95.3 ± 3.2, and 110.6 ± 3.4 kcal/mol, respectively). The cycloaromatization of *cis*-3-hexene-1,5-diyne to *para*-benzyne (the Bergman cyclization) is calculated to be endothermic by 13 kcal/mol.

Introduction

Of the many different types of reactive organic intermediates, biradicals are perhaps the most elusive. Although they are often invoked in pyrolytic and photochemical reaction mechanisms,[1,2] biradicals are nevertheless seldom observed because of their typically short lifetimes toward ring-closure reactions or because of their extreme bimolecular reactivity. Indirect evidence for biradical intermediates is often obtained from kinetic studies of stereomutation and rearrangement reactions of small ring compounds[3] and from trapping experiments with the decomposition products of cyclic and bicyclic azoalkanes.[4] Whereas biradicals are most often produced by ring-cleavage reactions, they can also be formed by certain electrocyclic reactions such as the Bergman cyclization[5] and its variants[6] that yield dehydroaromatic compounds. Recently, a new class of antitumor, antibiotic compounds has been discovered in which reactive dehydroaromatic biradicals produced by Bergman and Bergman-like cyclizations are believed to be responsible for the high biological activity.[7]

Despite their prevalence as intermediates in organic reactions, little is known about the thermochemical properties of biradicals because their high reactivity makes them difficult to characterize by conventional calorimetric and equilibrium techniques. Traditional methods for estimating biradical thermochemistry rely on the assumption of bond energy additivity; that is, the heat of formation of a biradical is usually estimated by using known C–H bond strengths in stable, closed-shell molecules in conjunction with an appropriate thermochemical cycle.[3,8] This approach obviously neglects interactions between the two radical centers in the biradical, interactions that could be either stabilizing or destabilizing. However, few experimental measurements of absolute heats of formation for biradicals are available with which to evaluate the bond energy additivity assumption. Time-resolved photoacoustic calorimetry (PAC) has been used recently to estimate the heats of formation of Closs's diradical[9] (cyclopentane-1,3-diyl) and its 2-isopropylidene derivative.[10] The reported value for Closs's diradical is essentially identical to the bond strength additivity estimate. However, the PAC data contain unknown solvation energy and volume-change contributions, and the heat

• Abstract published in *Advance ACS Abstracts*, June 15, 1994.

(1) *Diradicals*; Borden, W. T., Ed.; Wiley: New York, 1982.

(2) (a) Turro, N. J. *Modern Molecular Photochemistry*; Benjamin/Cummings: Menlo Park, CA, 1978. (b) Dauben, W. G.; Salem. L.; Turro, N. J. *Acc. Chem. Res.* **1975**, *8*, 41. (c) Platz, M. S., Ed. *Kinetics and Spectroscopy of Carbenes and Biradicals*; Plenum Press: New York, NY, 1990.

(3) (a) Berson, J. A. In *Rearrangements in Ground and Excited States*; de Mayo, P., Ed.; Academic Press: New York, 1980; Vol. 1, p 311. (b) Bergman, R. G. In *Free Radicals*; Kochi, J. K., Ed.; Wiley: New York, 1973; Chapter 5. (c) O'Neal, H. E.; Benson, S. W. *J. Phys. Chem.* **1968**, *72*, 1866. (d) Baldwin, J. E.; Cianciosi, S. J.; Glenar, D. A.; Hoffman, G. J.; Wu, I.-W.; Lewis, D. K. *J. Am. Chem. Soc.* **1992**, *114*, 9408.

(4) Mackenzie, K. In *The Chemistry of the Hydrazo. Azo. and Azoxy Groups*, Patai, S., Ed.; Wiley: London, 1975; Part 1, Chapter 11. See also: Dervan, P. B.; Dougherty, D. A., in ref 1, Chapter 3.

(5) (a) Jones, R. R.; Bergman, R. G. *J. Am. Chem. Soc.* **1972**, *94*, 660. (b) Lockhart, T. P.; Comita, P. B.; Bergman, R. G. *J. Am. Chem. Soc.* **1981**, *103*, 4082.

(6) Myers, A. G.; Dragovich, P. S.; Kuo, E. Y. *J. Am. Chem. Soc.* **1992**, *114*, 9369, and references therein.

(7) (a) Lee, M. D.; Dunne, T. S.; Siegel, M. M.; Chang, C. C.; Morton, G. O.; Borders, D. B. *J. Am. Chem. Soc.* **1987**, *109*, 3464. Lee, M. D.; Dunne, T. S.; Chang, C. C.; Ellestad, G. A.; Siegel, M. M.; Morton, G. O.; McGahren, W. J.; Borders, D. B. *J. Am. Chem. Soc.* **1987**, *109*, 3466. (b) Golik, J.; Clardy, J.; Dubay, G.; Groenewold, G.; Kawaguchi, H.; Konishi, M.; Krishnan, B.; Ohkuma, H.; Saitoh, K.-i.; Doyle, T. W. *J. Am. Chem. Soc.* **1987**, *109*, 3461. Golik, J.; Dubay, G.; Groenewold, G.; Kawaguchi, H.; Konishi, M.; Krishman, B.; Ohkuma, H.; Saitoh, K.-i.; Doyle, T. W. *J. Am. Chem. Soc.* **1987**, *109*, 3462. (c) Konishi, M.; Ohkuma, H.; Tsuno, T.; Oki, T. *J. Am. Chem. Soc.* **1990**, *112*, 3715. (d) Zein, N.; Sinha, A. M.; McGahren, W. J.; Ellestad, G. A. *Science* **1988**, *240*, 1198.

(8) (a) Koga, N.; Morokuma, K. *J. Am. Chem. Soc.* **1991**, *113*, 1907. (b) Doering, W. v. E. *Proc. Natl. Acad. Sci. U.S.A.* **1981**, *78*, 5279. (c) O'Neal, H. E.; Benson, S. W. *Int. J. Chem. Kinet.* **1970**, *2*, 423.

(9) Buchwalter, S. L.; Closs, G. L. *J. Am. Chem. Soc.* **1975**, *97*, 3857. *Ibid* **1979**, *101*, 4688.

(10) Herman, M. S.; Goodman, J. L. *J. Am. Chem. Soc.* **1988**, *110*, 2681.

0002-7863/94/1516-6401$04.50/0

Scheme 1

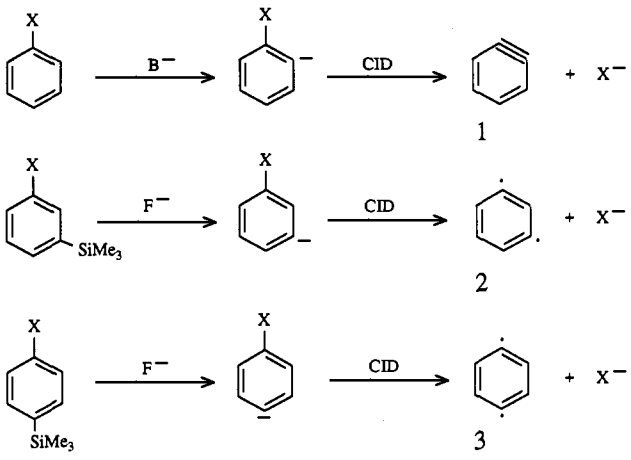

of formation derived for 2-isopropylidenecyclopentane-1,3-diyl ultimately relies on empirical estimates for some of the auxilliary thermochemical data. Most previous studies of biradical thermochemistry in the literature pertain to the archetypal dehydroaromatic 1,2-biradical, *ortho*-benzyne. The reported values for its gas-phase heat of formation lie in the range 100–118 kcal/mol. Various experimental approaches for *ortho*-benzyne have been employed, most of which are based upon a thermochemical cycle that combines either an ionization potential with an appearance energy,[11,12,13] an electron affinity with a gas-phase acidity,[14] or an appearance energy with a proton affinity.[15] Riveros et al. recently described a gas-phase ion/molecule reaction strategy for estimating the heat of formation of *ortho*-benzyne.[16] The results of these various determinations have been summarized by Guo and Grabowski.[14]

We recently reported measurements of absolute heats of formation for *ortho*-, *meta*-, and *para*-benzyne, (**1**, **2**, and **3**, respectively), which were determined from the apparent threshold energies for collision-induced dissociation (CID) of the corresponding isomeric chlorophenyl anions generated in a flowing afterglow–triple quadrupole instrument (Scheme 1, X = Cl).[17] The value obtained for *ortho*-benzyne, $\Delta H°_{f,298}(\mathbf{1}) = 106 \pm 3$ kcal/mol, is in excellent agreement with two recent determinations by independent experimental methods: 105 ± 3 kcal/mol obtained from ion/molecule reaction bracketing experiments by Riveros et al.[16] and 105 ± 5 kcal/mol from a determination of the gas-phase acidity of phenyl radical by Guo and Grabowski.[14] The CID threshold energies obtained with *meta*- and *para*-chlorophenyl anions, when combined with their proton affinities determined by a bracketing procedure, gave the values $\Delta H°_{f,298}(\mathbf{2}) = 116 \pm 3$ kcal/mol and $\Delta H°_{f,298}(\mathbf{3}) = 128 \pm 3$ kcal/mol. Although there are no prior experimental measurements with which to compare the data for **2** and **3**, the apparent stability ordering, $\Delta H_f(\mathbf{1}) < \Delta H_f(\mathbf{2}) < \Delta H_f(\mathbf{3})$, and the measured differences in the heats of formation are consistent with earlier theoretical predictions based on GVB calculations.[18] A useful perspective for the measured heats of formation for **1**–**3** can be obtained by comparing them to the value predicted by simple bond energy additivity. Using a value for $DH_{298}[C_6H_5\text{-}H] = 111.2 \pm 0.8$ kcal/mol (*vide infra*) along with the well-established heat of formation for benzene, a heat of formation for C_6H_4 of 137.9 ± 1.1 kcal/mol can be derived, indicating relative stabilization energies for **1**, **2**, and **3** of 32, 22, and 10 kcal/mol, respectively. In attempting to understand the origins of these apparent stabilization energies, our group[19] and, independently, Nicolaides and Borden[20] and Kraka and Cremer[21] carried out high-level *ab initio* calculations of the structures, energies, and singlet–triplet splittings for the three benzyne isomers. As summarized in these publications, CI calculations support the experimental value for $\Delta H_f(\mathbf{1})$, but provide convincing evidence that the measured heats of formation for **2** and **3** are both too low by 8–10 kcal/mol.

In this paper we present the complete details of our earlier thermochemical measurements for *ortho*-, *meta*- and *para*-benzyne,[17] along with revised values for their heats of formation based on new measurements. In seeking an explanation for the apparent failure of the previous measurements for **2** and **3**, but their success for **1**, we discovered a rather subtle contamination problem that had a significant influence on both the CID threshold measurements and the anion proton affinity determinations involving the *meta*- and *para*-chlorophenyl anions. We will show how deuterium-labeling provides a means to overcome this contamination problem and thereby permits the determination of CID thresholds for the isomerically pure chlorophenyl anions. Revised proton affinity measurements are also described for *meta*- and *para*-chlorophenyl anions using an alternative experimental procedure than the one used previously. The new values for ΔH_f(**2**) and ΔH_f(**3**) derived from these revised measurements are shown to be in excellent agreement with the theoretically predicted values.

Experimental Section

All experiments were carried out with a flowing afterglow–triple quadrupole apparatus that has been described in detail previously.[22,23] Unless otherwise noted, the standard operating conditions used were P(He) = 0.4 Torr, flow(He) = 200 STP cm³/s, and velocity(He) = 9400 cm/s. Primary reactant ions are generated by electron ionization of pure gases added near an electron emission source located at the upstream end of the flow tube. For the present experiments, OH^- was generated by electron ionization of a mixture of N_2O and CH_4, NH_2^- was made from NH_3, and F^- was formed by ionization of either NF_3 or CF_4. The primary ions are transported by the helium through the 100 cm × 7.3 cm i.d. flow reactor, where they are allowed to react with neutral reagent gases introduced at various positions through metered inlets. *Ortho*-halophenyl anions, $XC_6H_4^-$, X = F, Cl, Br, were prepared by proton abstraction from the corresponding halobenzene with OH^- and, in the case of chlorobenzene, with the conjugate base anion of furan ($C_4H_3O^-$). Furanide ion was, in turn, generated from the reaction of OH^- and NH_2^- with furan. The *meta*- and *para*-halophenyl anions were prepared using the DePuy fluoride-induced desilylation procedure,[24] i.e., by reaction of F^- with the corresponding *meta*- and *para*-(halophenyl)trimethylsilanes (Scheme 1). The ions in the flow tube are thermalized to ambient temperature (*ca.* 298 K) by up to 10^5 collisions with the helium buffer gas prior to sampling. Ions are gently extracted from the flow tube through a 0.5-mm orifice in a nose cone and focused into an EXTREL triple quadrupole mass analyzer. For collision-induced dissociation studies, the ion of interest is selected with the first quadrupole (Q1) and then injected with variable kinetic energy into the second quadrupole (Q2; radio frequency only), which serves as a gas-tight collision chamber. Argon collision gas was

(11) Grützmacher, H.-F.; Lohmann, J. *Justus Liebigs Ann. Chem.* **1967**, *705*, 81.
(12) Rosenstock, H. M.; Stockbauer, R.; Parr, A. C. *J. Chim. Phys.* **1980**, *77*, 745.
(13) Moini, M.; Leroi, G. E. *J. Phys. Chem.* **1986**, *90*, 4002.
(14) Guo, Y.; Grabowski, J. J. *J. Am. Chem. Soc.* **1991**, *113*, 5923.
(15) Pollack, S. K.; Hehre, W. J. *Tetrahedron Lett.* **1980**, *21*, 2483.
(16) Riveros, J. M.; Ingemann, S.; Nibbering, N. M. M. *J. Am. Chem. Soc.* **1991**, *113*, 1053.
(17) Wenthold, P. G.; Paulino, J. A.; Squires, R. R. *J. Am. Chem. Soc.* **1991**, *113*, 7414.
(18) Noell, O. J.; Newton, M. D. *J. Am. Chem. Soc.* **1979**, *101*, 51.
(19) Wierschke, S. G.; Nash, J. J.; Squires, R. R. *J. Am. Chem. Soc.* **1993**, *115*, 11958. The predicted heats of formation for **1**, **2**, and **3** quoted in the present work differ slightly from those reported in the original paper due to the use of a different value for the C–H bond strength in benzene; see text for discussion.
(20) Nicolaides, A.; Borden, W. T. *J. Am. Chem. Soc.* **1993**, *115*, 11951.
(21) Kraka, E.; Cremer, D. *Chem. Phys. Lett.* **1993**, *216*, 333. Kraka, E.; Cremer, D. *J. Am. Chem. Soc.*, in press.
(22) Graul, S. T.; Squires, R. R. *Mass Spectrom. Rev.* **1988**, *7*, 1.
(23) Marinelli, P. J.; Paulino, J. A.; Sunderlin, L. S.; Wenthold, P. G.; Poutsma, J. C.; Squires, R. R. *Int. J. Mass. Spectrom. Ion Processes* **1994**, *130*, 89.
(24) DePuy, C. H.; Bierbaum, V. M.; Flippin, L. A.; Grabowski, J. J.; King, G. K.; Schmitt, R. J.; Sullivan, S. A. *J. Am. Chem. Soc.* **1979**, *101*, 6443.

used for all CID experiments reported in this study except *ortho*-bromophenyl anion. Neon was used as a collision gas for this ion in order to minimize broadening of the low-energy dissociation onset. The pressure in the collision region is kept below 5×10^{-5} Torr to minimize the effects of secondary ion–target collisions on the product ion appearance curves.[23] The ion axial kinetic energy in Q2 is determined by the quadrupole rod offset voltage, which can be varied over the range 0–200 V. Reactant and product ions are mass-selected with the third quadrupole (Q3), and then detected with an electron multiplier operated in pulse-counting mode.

Collision-Induced Dissociation Threshold Energy Measurements. Detailed descriptions of the data collection and analysis procedures used for CID threshold measurements with the flowing afterglow–triple quadrupole apparatus have been published elsewhere.[25-28] The normalized product ion yield or partial cross section for CID of the mass-selected reactant ion is monitored while the Q2 rod offset voltage is scanned. The ion/target collision energy in the center-of-mass frame (E_{CM}) is given by eq 1, where E_{lab} is the nominal lab energy, M is the mass of the

$$E_{CM} = E_{lab}[m/(M + m)] \quad (1)$$

reactant ion, and m is the mass of the neutral target. For the experiments with *ortho*-bromophenyl anion using neon, an effective target mass of 20.2 amu was used (the weighted average of the natural isotope abundances). Determination of the ion kinetic energy origin and beam energy spread is accomplished by retarding potential analysis, with Q2 serving as the retarding field element. Ion beam energy distributions are found to be approximately Gaussian in shape, with a typical full width at half-height of 0.5 –1.5 eV (laboratory frame).

Absolute cross sections for CID (σ_p) are calculated using $\sigma_p = I_p/INl$, where I_p and I are the intensities of the product and reactant ions, respectively, N is the number density of the target gas, and l is the effective collision path length. This relationship is valid as long as the target number density is kept sufficiently low that the total extent of dissociation is less than *ca.* 5%. The effective path length in the collision cell is measured to be 24 ± 4 cm on the basis of calibration with the known[29] cross section for the reaction $Ar^+ + D_2 \rightarrow ArD^+ + D$. The reported absolute cross sections are the average of multiple determinations, with estimated uncertainties of ±50%. Relative cross sections are more accurate, with estimated uncertainties of ±20%.

A plot of the normalized product ion yield or CID cross section versus E_{CM} gives an ion appearance curve from which the activation energy for dissociation can be derived. This is accomplished by fitting the data with a model threshold law that is convoluted with certain distribution functions that can cause broadening of the dissociation onset. The simplest form of the model threshold law—the one employed in our previous study[17]—is shown in eq 2, where $\sigma(E)$ is the cross section at energy E, E_T is the

$$\sigma(E) = \sigma_0(E - E_T)^n/E \quad (2)$$

threshold energy, σ_0 is a scaling factor, and n is an adjustable parameter.[30] Analysis is carried out by an iterative procedure in which σ_0, n, and E_T are varied so as to minimize the deviation between the steeply rising portions of the calculated and experimental appearance curves.[31] The region near the reaction onset is not included in the fit due to tailing in the data obtained from our instrument that is attributed to fragmentation caused by collisional activation of the reactant ion in the vicinity of the electrostatic lenses flanking Q2 and/or within the first and third quadrupoles. Attempts to fit the experimental data in the threshold region lead to very high values for the exponent n and unreasonably low (near 0 eV) values for the dissociation activation energy. Convoluted with the trial excitation function are the reactant ion kinetic energy distribution, approximated by a Gaussian function with a 1.5-eV width, and a Doppler broadening function developed by Chantry[32] to account for random thermal motion of the neutral target. The threshold energy determined in this manner is considered to correspond to an activation energy for dissociation of room-temperature (298 K) reactant ions to room-temperature products, i.e., ΔE_{298}.[27,28]

In the present study, we have also examined the potential effects on the derived CID thresholds of the reactant ion thermal energy and the "kinetic shift" that could accompany slow unimolecular decomposition. A more complete model threshold law for CID reactions that explicitly accounts for these two factors, similar to that developed by Armentrout and co-workers,[33] is shown in eq 3. Here, i denotes reactant ion vibrational

$$\sigma(E) = \sigma_0 \sum_i [g_i P_D(E,E_i,\tau)(E + E_i - E_T)^n/E] \quad (3)$$

states having energy E_i and population g_i ($\Sigma g_i = 1$), and P_D is the probability that metastable ions formed with initial translational energy E and internal energy E_i will dissociate within the experimental time window (*ca.* 30 μs, the estimated flight time from Q2 to Q3 of an activated ion in a "typical" CID reaction[23]). The rotational energy is assumed to be conserved in CID reactions, so it is not included in the model excitation function. The internal energy distributions of the halophenyl reactant ions were estimated from calculated vibrational frequencies obtained from semiempirical molecular orbital calculations using the MOPAC 6.0 package and the AM1 Hamiltonian.[34] The computed harmonic frequencies determined for each of the fully relaxed species were scaled by a factor of 0.9.[35] The dissociation probabilities, P_D, were obtained by calculating the unimolecular decay rate as a function of reactant ion internal energy in accordance with the RRKM prescription.[36] For this analysis, the density of states for the reactant ions was obtained from the scaled molecular vibrational frequencies. For the dissociation transition states, the frequencies computed for each separate benzyne molecule were combined with several different trial sets of two low frequencies in the range 10–350 cm^{-1} to represent the two nondegenerate carbon–halide bending modes. These bends have frequencies in the 200–530 cm^{-1} range in the reactant bromo- and chlorophenyl anions. The modified threshold law given by eq 3 is then convoluted with the ion beam energy distribution and Doppler broadening functions and iteratively fit to the steeply rising portion of the ion appearance curve, as described above. Because of the explicit inclusion of the reactant ion thermal energy content in the fitting procedure, the CID threshold energy obtained in this way is considered to correspond to the 0 K dissociation energy, i.e., ΔE_0. The corresponding ΔE_{298} values are obtained by adding the difference in integrated heat capacities for the products and reactants (also obtained from semiempirical MO calculations[34]). For deriving heats of formation, an additional factor of RT (0.59 kcal/mol at 298 K), corresponding to the PV work term for dissociation, is also added to convert ΔE_{298} to an enthalpy change.

Materials. The (halophenyl)trimethylsilanes, (halophenyl)dimethylphenylsilanes, and the deuterated (halophenyl)trimethylsilanes were prepared from the reaction of the corresponding halophenyl Grignard reagent or halophenyllithium species with the appropriate chlorosilane.[37] The Grignard and organolithium reagents were, in turn, prepared from the corresponding dichloro-, dibromo-, or bromochlorobenzenes. *meta*-Bromochlorobenzene-d_4 and *meta*-dibromobenzene-d_4 were prepared by catalytic H/D exchange of the undeuterated materials.[38] *para*-Dichlorobenzene-d_4 (98% d_4), *para*-dibromobenzene-d_4 (98% d_4), and chlorobenzene-d_5 (98% d_5) were obtained from Aldrich. *meta*-Dichlorobenzene-d_4 (98% d_4) was obtained from C/D/N Isotopes. Other reagents were obtained from commercial suppliers, and all liquid samples were degassed prior to use. Gas purities were as follows: He (99.995%), Ar (99.955%), Ne (99.999%), N_2O (99%), CH_4 (99%), NF_3 (98%), CF_4 (99.99%).

(25) Graul, S. T.; Squires, R. R. *J. Am. Chem. Soc.* **1990**, *112*, 2517.
(26) (a) Paulino, J. A.; Squires, R. R. *J. Am. Chem. Soc.* **1991**, *113*, 1845. (b) Paulino. J. A.; Squires, R. R. *J. Am. Chem. Soc.* **1991**, *113*, 5573.
(27) Sunderlin, L. S.; Wang, D.; Squires, R. R. *J. Am. Chem. Soc.* **1992**, *114*, 2788.
(28) Sunderlin, L. S.; Wang, D.; Squires, R. R. *J. Am. Chem. Soc.* **1993**, *115*, 12060.
(29) Ervin, K. M.; Armentrout, P. B. *J. Chem. Phys.* **1985**, *83*, 166.
(30) (a) Chesnavich, W. J.; Bowers, M. T. *J. Phys. Chem.* **1979**, *83*, 900. (b) Sunderlin, L. S.; Armentrout, P. B. *Int. J. Mass Spectrom. Ion Processes* **1989**, *94*, 149, and references therein.
(31) Analysis carried out using the CRUNCH program written by Prof. P. B. Armentrout and co-workers.
(32) Chantry, P. J. *J. Chem. Phys.* **1971**, *55*, 2746.
(33) (a) Schultz, R. H.; Crellin, K. C.; Armentrout, P. B. *J. Am. Chem. Soc.* **1991**, *113*, 8590. (b) Khan, F. A.; Clemmer, D. E.; Schultz, R. H.; Armentrout, P. B. *J. Phys. Chem.* **1993**, *97*, 7978.
(34) AM1: Dewar, M. J. S.; Zoebisch, E. G.; Healy, E. F.; Stewart, J. J. P. *J. Am. Chem. Soc.* **1985**, *107*, 3902. MOPAC: Stewart, J. J. P., QCPE No. 455.
(35) Hout, R. F., Jr.; Levi, B. A.; Hehre, W. J. *J. Comput. Chem.* **1982**, *3*, 234.
(36) Robinson, J. P.; Holbrook, K. A. *Unimolecular Reactions*; Wiley-Interscience: New York, 1972. Forst, W. *Theory of Unimolecular Reactions*; Academic: New York, 1973.
(37) (a) Clark, H. A.; Gordon, A. F.: Young, C. W., Hunter, M. J. *J. Am. Chem. Soc.* **1951**, *73*, 3798. (b) Klusener, P. A. A.; Hanekamp, J. C.; Brandsma, L.; Schleyer, P. v. R. *J. Org. Chem.* **1990**, *55*, 1311.
(38) Long, M. A.; Garnett, J. L.; Vining, R. F. W. *J. Chem. Soc., Perkin Trans. 2* **1975**, 1298.

Table 1. Supplemental Thermochemical Data

compound	$\Delta H°_{f,298}$(g), kcal/mol	ref
C_6H_5Cl	13.0 ± 0.2	*a*
HCl	−22.1 ± 0.04	*b*
C_6H_5Br	24.9 ± 0.7	*c*
HBr	−8.7 ± 0.1	*b*
C_6H_6	19.7 ± 0.2	*c*
C_6H_5	78.9 ± 0.8	see text
H	52.1	*b*
H^+	365.7	*d*
	ΔH_{acid}, kcal/mol	ref
HCl	333.4 ± 0.2	*d*
HBr	323.6 ± 0.3	*d*

[a] Platanov, V. A.; Simulin, Y. N. *Russ. J. Phys. Chem.* **1985**, *59*, 179. [b] Reference 49. [c] Pedley, J. B.; Rylance, J. *Sussex-N.P.L. Computer Analysed Thermochemical Data: Organic and Organometallic Compounds*; University of Sussex, 1977. [d] Reference 47.

Results and Discussion

The experimental approach used here for determining absolute heats of formation for the benzynes represents a natural extension of the methods developed previously for carbenes.[26] We have shown that accurate carbene thermochemistry can be obtained from analysis of the energetics of halide ion dissociation from α-halocarbanions, i.e., from α-elimination reactions. For biradicals, the energetics for "α,ω-elimination" of a halide ion from a structurally and thermochemically well-defined halocarbanion must be determined. Thus, in order to obtain absolute heats of formation for *ortho*-, *meta*-, and *para*-benzyne, the three corresponding halophenyl anion isomers must be generated in pure form and the threshold energies for halide dissociation determined (Scheme 1). The measured activation energy (E_T) can be directly equated with the corresponding bond dissociation energy, provided that halide dissociation occurs rapidly on the experimental time scale, i.e., no "kinetic shift" in the reaction onset, and that the reverse process (addition of a halide ion to a benzyne) has a negligible energy barrier.[39] The heat of formation of the benzyne product of the dissociation can then be derived from the measured value of E_T and other thermochemical data according to eq 4, where $\Delta H_{acid}(C_6H_5X)$ is the appropriate gas-

$$\Delta H°_{f,298}(C_6H_4) = E_T + K + \Delta H_{acid}(C_6H_5X) + \Delta H°_{f,298}(C_6H_5X) - \Delta H_{acid}(HX) - \Delta H°_{f,298}(HX) \quad (4)$$

phase acidity of the halobenzene precursor, and the data for the remaining three enthalpy terms are all well-known (Table 1). The term K is required to convert E_T (=ΔE) to a bond dissociation enthalpy. With the CID threshold model shown in eq 2, which equates E_T with ΔE_{298}, K is simply given by the PV work term for the dissociation, RT (0.59 kcal/mol at 298 K). With the more elaborate model shown in eq 3, the 0 K dissociation energy is obtained (ΔE_0), so an additional factor given by the difference in the integrated heat capacities (0–298 K) for the products and reactants must be added.[40] Therefore, the principal measurements required for this approach are the CID threshold energies, E_T, and the gas-phase acidities of a halobenzene molecule in the *ortho*, *meta*, and *para* positions (or, equivalently, the proton affinities of the corresponding conjugate base anions). One advantage of this particular experimental method for determining benzyne thermochemistry is the flexibility with respect to the halide leaving group used for the α,ω-elimination. Thus, it is possible, in principle, to obtain up to four independent measurements of the heat of formation for each benzyne by examining the corresponding fluoro-, chloro-, bromo-, and iodophenyl anions.

(39) Baer, T. *Adv. Chem. Phys.* **1986**, *64*, 111, and references therein.
(40) Traeger, J. C.; McLoughlin, R. G. *J. Am. Chem. Soc.* **1981**, *103*, 3647.

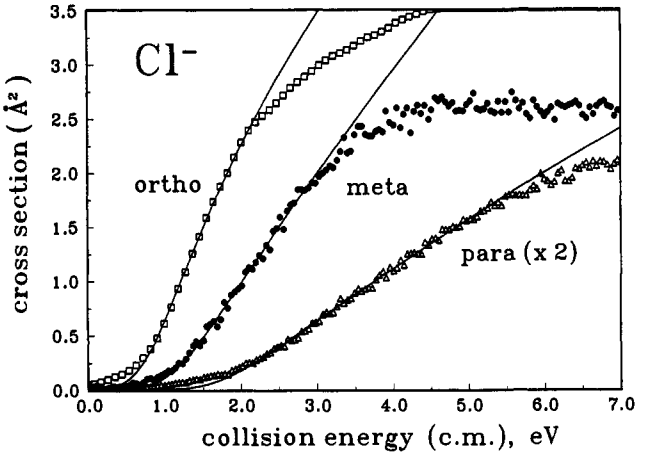

Figure 1. Cross sections for collision-induced dissociation of Cl^- from *ortho*-, *meta*-, and *para*-chlorophenyl anions as a function of translational energy in the center-of-mass frame. The solid lines are the model appearance curves calculated using eq 2, convoluted as discussed in the text.

In the following sections, we first describe the formation, identification, and energy-resolved CID of a series of isomeric halophenyl anions (X = F, Cl, Br), along with their apparent acid–base behavior determined by standard bracketing procedures. We next demonstrate how acid-catalyzed isomerization of *meta*- and *para*-halophenyl anions in the flowing afterglow leads to erroneous CID thresholds and proton affinities and how the use of deuterium-substituted precursors and an alternative method for evaluating the basicities of halophenyl anions leads to new values for the benzyne heats of formation that are consistent with theoretical predictions.[19,20] Finally, we present a brief discussion of the implications of the experimental thermochemistry obtained in this way for the benzynes.

Ion Formation and Structural Studies. Initial measurements[17] of the heats of formation for **1**, **2**, and **3** were obtained by measuring the thresholds for chloride elimination from *ortho*-, *meta*-, and *para*-chlorophenyl anions (Scheme 1, X = Cl). Chlorophenyl anions are readily prepared in the gas phase by proton abstraction from chlorobenzene by OH^- and other stronger bases. However, because of the expected similarity of the gas-phase acidities of the three different ring positions,[41] regioselective ion synthesis procedures must be employed. The conjugate base anion of furan (furanide ion) has been found to deprotonate chlorobenzene exclusively at the *ortho* position (*vide infra*). For the *meta* and *para* isomers, fluoride-induced desilylation was used.[24] Reaction of F^- ion with purified samples of *meta*- and *para*-(chlorophenyl)-trimethylsilane yields abundant signals of chlorophenyl anion products.

Preliminary indications that the chlorophenyl anions formed by the above procedures had the expected isomeric structures came from their characteristic energy-resolved CID behavior. All three chlorophenyl anions undergo efficient fragmentation upon collisional activation with argon target in the triple quadrupole analyzer to give chloride as the only ionic product. The energy-dependent CID cross sections measured for these ions are shown in Figure 1. Three distinct Cl^- appearance curves are evident that display marked differences in both the maximum CID cross sections and the apparent dissociation onsets. For *ortho*-, *meta*-, and *para*-chlorophenyl anions, the measured maximum CID cross sections in the 5–7 eV (CM) range are 3.6, 2.6, and 1.0 Å², respectively, while the approximate thresholds obtained by simple linear extrapolation of the steeply rising portions of the appearance curves are *ca.* 0.6, 1.0, and 1.5 eV (CM), respectively. Thus, the occurrence of three distinct CID cross sections suggests the formation of different populations of reactant ions from the different neutral precursors.

(41) Meot-Ner, M.; Kafafi, S. A. *J. Am. Chem. Soc.* **1988**, *110*, 6297.

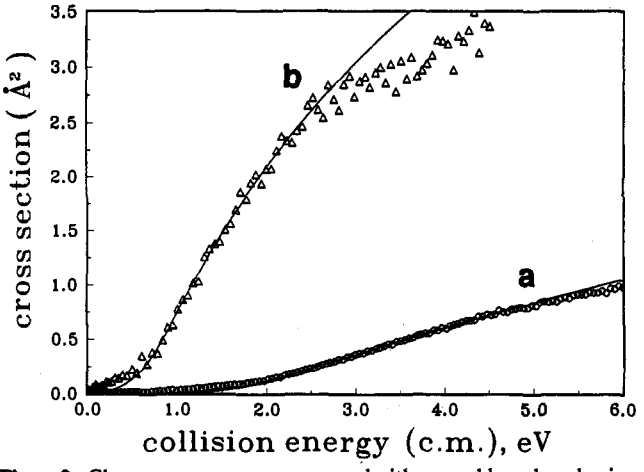

Figure 2. Cl^- appearance curves measured with *para*-chlorophenyl anion (a) in a "dry" flow tube and (b) with *ca.* 0.01 STP cm^3/s H_2O added to the flow tube.

Additional support for the formation of three isomeric chlorophenyl anions from the different precursors is obtained from the fact that they can be chemically interconverted. Addition of water vapor to the flow tube through a downstream gas inlet leads to significant changes in the measured Cl^- appearance curves obtained from CID of both the *meta*- and *para*- but not the *ortho*-chlorophenyl anions. For example, Figure 2 shows the Cl^- appearance curves measured for *para*-chlorophenyl anion with a "dry" flow tube (curve a) and with *ca.* 0.01 STP cm^3/s added H_2O (curve b). Significant shifts in both the maximum CID cross section and the apparent dissociation onset are evident, from roughly 1.0 $Å^2$ and 1.5 eV for the ion before reaction to *ca.* 3.5 $Å^2$ and 0.6 eV after addition of water, resulting in an appearance curve that is essentially the same as the one obtained from the *ortho* isomer. Similar behavior is observed with the *meta*-chlorophenyl anion: the initial Cl^- appearance curve becomes identical to the one for the *ortho*-chlorophenyl anion upon addition of water to the flow tube. This behavior is attributed to a water-catalyzed isomerization of both the *meta*- and *para*-chlorophenyl anions to the *ortho* isomer taking place in the flow tube prior to energy-resolved CID analysis. A plausible mechanism for this transformation is shown in Scheme 2 for the *para* isomer. Protonation of the *para*-chlorophenyl anion by H_2O results in an electrostatically bound [HO^-/chlorobenzene] complex that can dissociate to separated products (*vide infra*) or may have sufficient lifetime prior to dissociation to undergo a second proton transfer back to HO^- from the more acidic *ortho* position.[42] The net result is the catalytic isomerization of *para*-chlorophenyl anion to the *ortho* isomer, which would naturally lead to the observed changes in CID behavior of the ions sampled into the triple quadrupole analyzer. The relative ease whereby the three chlorophenyl anion isomers can interconvert *in the presence of water* is also clearly evident from the occurrence of four facile H/D exchanges in all three anions when they are allowed to react with D_2O in the flow reactor.[43]

The behavior of the corresponding bromophenyl anions is similar (Scheme 1, X = Br). Figure 3 shows the characteristic Br^- appearance curves obtained from CID of the $C_6H_4Br^-$ ions produced by deprotonation of bromobenzene with HO^- (giving the *ortho*-bromophenyl anion) and by fluoride-induced desilylation of *meta*- and *para*-(bromophenyl)trimethylsilane. Again, three distinct dissociation onsets and maximum CID cross sections are evident, suggesting the presence of three different populations of bromophenyl anions. The approximate thresholds estimated from simple linear extrapolation are roughly 0.3, 0.6, and 1.2 eV, and the maximum CID cross sections in the 4–6 eV (CM) collision energy range are *ca.* 8, 7, and 5 $Å^2$ for the *ortho*-, *meta*-, and *para*-bromophenyl anions, respectively. The lower dissociation thresholds and the higher associated CID cross sections relative to the chlorophenyl anions are a natural consequence of the weaker covalent and electrostatic binding of a bromide ion compared to a chloride ion.

As with the chlorophenyl anions, addition of water to the flow tube causes the higher threshold, lower yield Br^- appearance curves for the *meta* and *para* isomers to convert to the lower threshold, higher yield appearance curve associated with the *ortho* isomer. However, unlike the chlorophenyl anions, the bromophenyl anions show mainly signal attenuation when water is added, and high yields of $Br^-(H_2O)$ and other Br^--containing cluster species are produced. This is due to the extreme lability of the *ortho*-bromophenyl anion toward Br^- transfer, a fact that was clearly demonstrated in an earlier study by Riveros and co-workers of the gas-phase negative ion chemistry of bromobenzene.[16,44] Extensive signal depletion upon addition of D_2O prevented meaningful characterization of the H/D exchange behavior of the bromophenyl anions under the present conditions.

The behavior of fluorophenyl anions upon collisional activation is qualitatively and quantitatively different from that of the chloro- and bromophenyl anions. *Ortho*-fluorophenyl anions are readily prepared by deprotonation of fluorobenzene by HO^-. However, CID of this ion produces mainly the dehydrophenyl anion, $C_6H_4^-$, by loss of an HF molecule[45] with an apparent onset at *ca.* 2.0 eV. Fluoride is observed as a minor product of this reaction, with a maximum cross section on the order of 0.1 $Å^2$, but with an appearance curve characterized by a slowly rising onset with an apparent threshold energy of *ca.* 5 eV, much higher than would be expected for direct dissociation to F^- + **1** (≈2.2 eV, *vide infra*). The unusually high threshold observed for F^- formation may be the result of a "competitive shift"[46] caused by the presence of the more efficient HF-loss channel or by collision-induced electron detachment from the *ortho*-fluorophenyl anion. Note that, unlike the corresponding chloro- and bromo-derivatives, the *ortho*-fluorophenyl anion has an expected activation energy for halide loss that is significantly greater than the predicted electron binding energy of the reactant ion (*ca.* 1.5 eV, *vide infra*). A similarly high threshold energy (>5 eV) and low yield for F^- loss is observed when *para*-fluorophenyl anion (made by fluoride-induced desilylation of the corresponding trimethylsilyl precursor) is examined by energy-resolved CID. However, unlike the *ortho* isomer, *para*-fluorophenyl anion exhibits no HF loss, even at collision energies as high as 20 eV (CM). This suggests that the unusually high thresholds for F^- loss are probably not due to a competitive shift caused by HF loss, but more likely result from suppression of the total CID cross sections due to fast electron detachment from the precursors. The *meta*-fluorophenyl anion was not examined.

Acid–Base Bracketing Measurements. In order to calculate heats of formation for the benzynes using CID threshold energies, the heats of formation for the precursor halophenyl anions are required. These can be determined from the measured gas-phase acidities of the corresponding halobenzene molecules in the *ortho*, *meta*, and *para* positions. In our earlier study involving the chlorobenzenes, this was accomplished with use of bracketing techniques. The results of these experiments are summarized in Table 2. Hydroxide ion, deprotonated pyridine, and the conjugate base anion of furan are all observed to deprotonate chlorobenzene, while methoxide ion and other weaker base anions do not. Furthermore, *ortho*-chlorophenyl anions prepared by reaction of chlorobenzene with furanide ion are observed to deprotonate methanol and other stronger acids but do not deprotonate either

(42) Squires, R. R.; Bierbaum, V. M.; Grabowski, J. J.; DePuy, C. H. *J. Am. Chem. Soc.* **1983**, *105*, 5185, and references therein.
(43) Stewart, J. H.; Shapiro, R. H.; DePuy, C. H.; Bierbaum, V. M. *J. Am. Chem. Soc.* **1977**, *99*, 7650.
(44) Linnert, H. V.; Riveros, J. M. *J. Chem. Soc., Chem. Commun.* **1993**, 48.
(45) Gronert, S.; DePuy, C. H. *J. Am. Chem. Soc.* **1989**, *111*, 9253.
(46) Lifshitz, C.; Long, F. A. *J. Chem. Phys.* **1964**, *41*, 2468.

Scheme 2

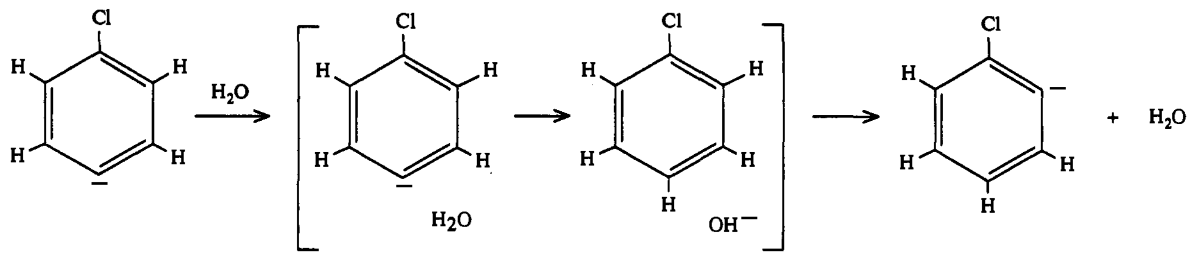

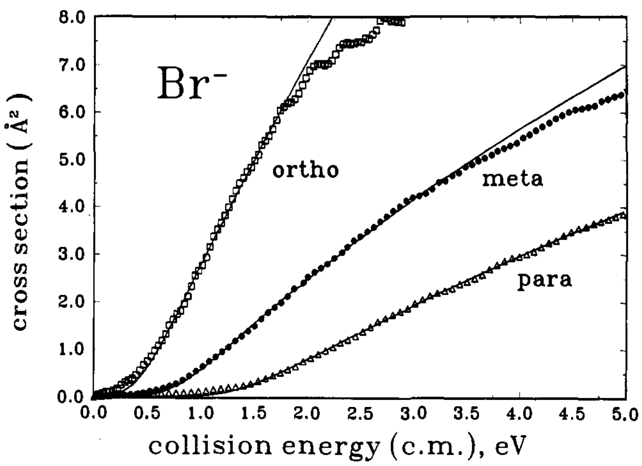

Figure 3. Cross sections for collision-induced dissociation of Br^- from *ortho*-, *meta*-, and *para*-chlorophenyl anions as a function of translational energy in the center-of-mass frame. The solid lines are the model appearance curves calculated using eq 2, convoluted as discussed in the text.

Table 2. Summary of Acid–Base Bracketing Experiments for the *Ortho*, *Meta*, and *Para* Positions of Chlorobenzene[a]

$$C_6H_4Cl^- + HA \rightleftarrows C_6H_5Cl + A^-$$

HA	$\Delta G_{acid}(HA)$[b]	*ortho* (forward)[c,d]	*ortho* (reverse)	*meta*[e]	*para*[e]
H_2O	384.1 ± 0.2	–	+	–	–
pyridine	382.7 ± 2.0	–	+	–	–
furan	380.0 ± 3.0	–	+	+	+
C_6H_5F	378.9 ± 2.0[f]	+ (fast)	+ (slow)	+	+
MeOH	374.0 ± 2.0	+	–	+	+

[a] All experiments carried out in the flowing afterglow at 298 K. [b] Values in kcal/mol; taken from ref 47 unless otherwise noted. [c] + and – correspond to observance and nonobservance of proton-transfer reaction, respectively. [d] By slow it is meant that while proton transfer is observed, it does so at an apparent rate that is less than that for the reverse proton-transfer reaction under conditions of comparable neutral flow. [e] Acidities for the *meta* and *para* positions were evaluated from reactions in the "forward" direction only. [f] Reference 41.

pyridine or furan. Reversible proton transfer occurs between *ortho*-chlorophenyl anion and fluorobenzene, indicating that the acidities of the *ortho* positions of chlorobenzene and fluorobenzene are similar. Although reaction rates were not measured, it is qualitatively apparent that proton transfer to *ortho*-chlorophenyl anion from fluorobenzene occurs more efficiently than does the reverse reaction. This suggests that fluorobenzene is slightly more acidic than chlorobenzene and, therefore, that the proton transfer from chlorobenzene to *ortho*-fluorophenyl anion is slightly endothermic. In contrast, the *meta*- and *para*-chlorophenyl anions prepared by fluoride-induced desilylation appear to be stronger bases. Both ions are observed to deprotonate methanol, fluorobenzene, and furan, while no *apparent* reaction occurs with either pyridine or H_2O (*vide infra*). As noted earlier, each of the chlorophenyl anions exchange up to four hydrogens for deuterium upon reaction with D_2O. However, OD^- is not observed as a primary product of any of these reactions. The results described above and listed in Table 2 indicate that the gas-phase acidity of the *ortho* position of chlorobenzene is between that of fluorobenzene (ΔG_{acid} = 378.9 ± 2.0 kcal/mol)[41] and furan (ΔG_{acid} = 380 ± 3 kcal/mol),[47] while the acidities of the *meta* and *para* positions are both between that of furan and pyridine (ΔG_{acid} = 382.7 ± 2.0 kcal/mol).[47] We therefore assign ΔG_{acid}(*ortho*-C_6H_5Cl) = 380.0 ± 2.0 kcal/mol, and ΔG_{acid}(*meta*-C_6H_5Cl) = ΔG_{acid}(*para*-C_6H_5Cl) = 382.0 ± 2.0 kcal/mol.

The $\Delta H_{acid}(C_6H_5Cl)$ terms needed for eq 4 can be calculated using $\Delta H_{acid} = \Delta G_{acid} + T\Delta S_{acid}$, where ΔS_{acid} refers to the entropy change for acid dissociation. These terms can be reasonably estimated from the relation $\Delta S_{acid} = \Delta S_{rot} + S(H^+)$,[48] where ΔS_{rot} is the change in rotational entropy and $S(H^+)$ is the absolute entropy of the proton (26.0 eu).[49] Deprotonation of chlorobenzene in either the *ortho* or *meta* position reduces the rotational symmetry number from 2 to 1, giving $\Delta S^\circ_{rot} = R \ln(2) = 1.4$ eu and ΔS_{acid} = 27.4 eu. Deprotonation in the *para* position does not change the rotational symmetry, so ΔS°_{rot} = 0.0 eu and ΔS_{acid} = 26.0 eu. Therefore, at 298 K the ΔH_{acid} values for the *ortho*, *meta*, and *para* positions of chlorobenzene are determined from the bracketing experiments to be 388.2 ± 2.0, 390.2 ± 2.0, and 389.7 ± 2.0 kcal/mol, respectively.

Riveros and co-workers have estimated the gas-phase acidity of bromobenzene in the *ortho* position to be slightly less than that of methanol, i.e., ΔH_{acid} = 382 kcal/mol.[16,44] Attempts to confirm this and to determine the proton affinities of the *meta*- and *para*-bromophenyl anions by bracketing procedures in the flowing afterglow were unsuccessful. Upon reaction of methanol with either the *ortho*-, *meta*-, or *para*-bromophenyl anions, the $C_6H_4Br^-$ signal disappears altogether without producing a significant amount of proton-transfer product. Instead, the major observed product ion is Br^-(MeOH), along with a lesser amount of free Br^- ion. Similar results are obtained from the reaction with water; that is, $Br^-(H_2O)$ and a small amount of free Br^- are the only detectable product ions. Consideration of the relative magnitudes of the Br^- binding energies of water and methanol (13 and 14 kcal/mol, respectively)[50] relative to the estimated values for *meta*- and *para*-bromophenyl anions (*ca.* 14 and 25 kcal/mol, cf. Figure 3) suggests that while direct Br^- transfer from the *meta* isomer to H_2O or MeOH is possible, Br^- transfer from *para*-bromophenyl anion should be endothermic. Therefore, the observed reactivity of the *meta*- and *para*-bromophenyl anions is probably due to a water- or methanol-catalyzed rearrangement of these ions to the *ortho* isomer by a mechanism similar to that shown in Scheme 2, followed by Br^- transfer to H_2O or MeOH prior to dissociation of the ion/molecule complex. The formation of free Br^- ion from these reactions could result from thermal dissociation of the weakly bound *ortho*-bromophenyl anion[16,44] or from CID of this labile species during sampling. Nevertheless, this behavior precludes

(47) Lias, S. G.; Bartmess, J. E.; Liebmann, J. F.; Holmes, J. L.; Levin, R. D.; Mallard, W. G. *J. Phys. Chem. Ref. Data* **1988**, *17*, Suppl. 1.
(48) Bartmess, J. E.; McIver, R. T., Jr. In *Gas Phase Ion Chemistry*; Bowers, M. T., Ed.; Academic Press: New York, 1979; Vol. 2, Chapter 11.
(49) Chase, M. W.; Davies, C. A.; Downey, J. R.; Frurip, D. J.; McDonald, R. A.; Syverud, A. N. *J. Phys. Chem. Ref. Data* **1985**, *14*, Suppl. 1 (JANAF Tables).
(50) (a) Burdett, N. A.; Hayhurst, A. N. *J. Chem. Soc.. Faraday Trans. 1* **1982**, *78*, 2997. (b) Hiraoka, K.; Yamabe, S. *Int. J. Mass Spectrom. Ion Processes* **1991**, *109*, 133.

bracketing experiments for determining the gas-phase acidities of the *ortho*, *meta*, and *para* positions of bromobenzene. However, compared to the corresponding positions in chlorobenzene, the *ortho* position of bromobenzene is reasonably expected to be slightly more acidic, while the *meta* and *para* positions should have about the same acidity.[41,47] On this basis we estimate ΔH_{acid} values for the *ortho*, *meta*, and *para* positions of bromobenzene of 387 ± 3, 390 ± 3, and 390 ± 3 kcal/mol, respectively. Because we were unable to obtain useful thresholds for CID of fluorophenyl anions, no attempts were made to determine positional acidities for fluorobenzene.

Analysis of CID Threshold Energies: Chloro- and Bromophenyl Anions. The threshold energies for dissociation of each of the chloro- and bromophenyl anion isomers were analyzed with use of eq 2 and, in order to account for potential effects of reactant ion internal energy and kinetic shifts, with use of the more elaborate model described by eq 3.

Shown in Figure 1 are the analytical fits of the CID cross sections for the three chlorophenyl anions obtained with use of eq 2. The linear portions of the appearance curves just above the reaction onsets were used for optimizing the fits, as described in the Experimental Section. The average fitting parameters obtained from many replicate measurements for each ion are $n = 1.63 \pm 0.10$ and $E_T = 15.7 \pm 1.6$, 24.2 ± 1.4, and 35.3 ± 1.4 kcal/mol for *ortho*-, *meta*-, and *para*-chlorophenyl anions, respectively, where the precision indicated is one standard deviation. Similarly, Figure 3 shows the fits obtained with eq 2 to the bromophenyl anion data using the optimized parameters: $n = 1.65 \pm 0.10$ and $E_T = 8.3 \pm 0.7$, 15.5 ± 0.8, and 27.4 ± 1.6 kcal/mol for *ortho*-, *meta*-, and *para*-bromophenyl anions, respectively. The similar n values obtained for the chloro- and bromophenyl anion data are consistent with the range of n values used for many other CID reactions.[25-28]

The observed onset for CID of a polyatomic ion can be affected by its natural thermal energy content and by the occurrence of slow unimolecular decomposition relative to the experimental time window.[28,33,36] The former effect, which will lower the apparent onset by an amount of energy roughly equal to the average internal energy of the reactant ion, can be evaluated from estimated vibrational frequencies. The latter effect, known as the "kinetic shift",[51] will increase the apparent onset by an amount of energy that depends upon the actual dissociation energy and on the number and type of internal degrees of freedom in the reactant ion. Kinetic shifts will be greatest for large molecules having high dissociation energies and many low-frequency vibrations, and smallest for relatively small or rigid molecules with weak bonds. To a first approximation, the effects of internal energy and kinetic shifts can be assumed to cancel, which is tantamount to assuming that the products of the CID reaction are formed at approximately the same temperature as the reactant ion. We have tested this assumption for the present systems by reanalyzing the threshold data with use of eq 3, which explicitly accounts for the reactant ion internal energy and for the effects of slow dissociation as modeled by RRKM calculations.

Using scaled, harmonic vibrational frequencies obtained from semiempirical molecular orbital calculations, the average internal energies of the chloro- and bromophenyl anions are calculated to be 1.7 and 1.8 kcal/mol, respectively (all three isomers are essentially the same). In order to evaluate the dissociation probability factors (P_D in eq 3), the densities of vibrational states for the reactant ion and the dissociation transition state must be known. For the reactant ions, the densities of states are reliably estimated from the computed molecular frequencies. Moreover, experience has shown that the RRKM results are not especially sensitive to the details of these frequency assignments. In contrast, the calculated RRKM lifetime effects can be extremely sensitive to the description of the dissociation transition state. We have examined several different transition state models possessing varying degrees of "tightness" or "looseness". This quality of the transition state is best reflected by the activation entropy for the dissociation reaction, $\Delta S^{\ddagger}$. $\Delta S^{\ddagger}$ can be calculated from the vibrational frequencies of the reactant ion and assumed values for the transition state by means of the corresponding partition functions, Q and $Q^{\ddagger}$ (eq 5), where $q_i = 1/[1 - \exp(-h\nu/k_BT)]$ and

$$\Delta S^{\ddagger} = k_B \ln Q^{\ddagger}/Q + (E_v^{\ddagger} - E_v)/T = k_B \ln(\prod q_i^{\ddagger}/\prod q_i) + (E_v^{\ddagger} - E_v)/T \quad (5)$$

$E_v^{\ddagger}$ and E_v are the average vibrational energies of the transition state and the reactant ion, respectively. By convention, the activation entropies are evaluated at $T = 1000$ K. When $\Delta S^{\ddagger}_{1000} > 0$, the reaction is said to have a loose transition state, and if $\Delta S^{\ddagger}_{1000} < 0$, the reaction has a tight transition state.

In order to characterize the influence of different transition-state models, a representative *para*-chlorophenyl-d_4 anion data set was analyzed. The reasons for using data for a deuterated ion and the origins of the differences compared to undeuterated ion data are described in a later section. The representative data set was initially fit using eq 2 with $E_T = 1.83$ eV and $n = 1.45$. This same data set was then reanalyzed using eq 3. In the simplest approximation, the transition-state frequencies can be taken to be those of the reactant ion less one C–Cl stretch frequency corresponding to the reaction coordinate. This corresponds to a value for $\Delta S^{\ddagger}_{1000}$ of 0.0 eu. The optimized fit with this model gives $E_T = 1.67$ eV and $n = 1.43$. Compared to the E_T value obtained with use of eq 2, this indicates a net shift in the dissociation onset of 3.7 kcal/mol due to ion lifetime and internal energy effects. However, this transition state model is certainly too "tight", since the in-plane and out-of-plane C–Cl bending frequencies in the real dissociation transition state are bound to be considerably less than those in the reactant ion (*ca.* 350–500 cm^{-1}), perhaps by factors of 10 or more. Accordingly, we have analyzed the same *para*-chlorophenyl-d_4 anion data using two different types of alternative transition-state models in which the frequencies are taken to be (1) those of the reactant chlorophenyl anion minus the C–Cl stretch with reduced values for the C–Cl bends, referred to as the "$\nu_{react} - 1$" model, and (2) those of the neutral *para*-benzyne product (obtained from semiempirical MO calculations for the singlet states) plus two additional low frequencies to represent bending of the stretched C–Cl bond, referred to as the "ν_{prod}" model. These model parameters, including the bending frequencies used and the corresponding values for $\Delta S^{\ddagger}_{1000}$, are listed in Table 3 along with the resulting E_T and n values derived from the fits. For comparison, the $\Delta S^{\ddagger}_{1000}$ value for the related dissociation of bromobenzene cations by Br atom loss has been estimated from time-resolved photodissociation experiments to be *ca.* 8 eu,[52] and somewhat less for Cl atom loss from chlorobenzene cations.[53,54]

Large differences between $\Delta S^{\ddagger}_{1000}$ values derived from the $\nu_{react} - 1$ and ν_{prod} models for a given C–Cl bending frequency pair are evident. This indicates that the net differences in all the other molecular vibrational frequencies between a *para*-chlorophenyl anion and a neutral *para*-benzyne are having a significant influence. Thus, the central question becomes whether in the dissociation transition state the hydrocarbon moiety is more "reactant-like" or more "product-like". Model calculations using semiempirical MO methods suggest that the intramolecular vibrational frequencies associated with the C_6H_4 moiety in *para*-

(51) Levsen, K. *Fundamental Aspects of Organic Mass Specrometry*; Verlag Chemie: New York, 1978.

(52) Malinovich, Y.; Arakawa, R.; Haase, G.; Lifshitz, C. *J. Phys. Chem.* **1985**, *89*, 2253.

(53) Pratt, S. T.; Chupka, W. A. *Chem. Phys.* **1981**, 153.

(54) The threshold energy for CID of chlorobenzene cations is found to agree with the literature dissociation energy (3.3 eV[47]) when the CID data are modeled with eq 3 and parameters corresponding to $\Delta S^{\ddagger}_{1000} = 5.1$: Wenthold. P. G.; Squires, R. R. Unpublished results.

Table 3. Model Parameters Used for Analyzing Representative *para*-Chlorophenyl Anion Appearance Curve Using Eq 3 and Derived CID Threshold Energies

transition-state model	C–Cl bending frequencies, cm^{-1}	$\Delta S^{\ddagger}_{1000}$, eu[a]	E_T, n (eq 3)
$\nu_{react} - 1$[b]	368, 399[c]	0.0	1.67, 1.43
	350, 350	0.3	1.68, 1.43
	200, 200	2.3	1.71, 1.44
	100, 100	4.9	1.75, 1.44
	50, 50	7.6	1.79, 1.44
	10, 10	14.0	1.83, 1.49
ν_{prod}[d]	350, 350	−4.2	1.54, 1.43
	200, 200	−2.2	1.58, 1.44
	100, 100	0.5	1.62, 1.44
	50, 50	3.1	1.67, 1.44
	25, 25	5.9	1.72, 1.44
	15, 15	7.9	1.75, 1.44
	8, 8	10.4	1.78, 1.44

[a] Dissociation activation entropy as defined in eq 5. [b] Transition-state frequencies taken as the reactant frequencies less one C–Cl stretch with reduced C–Cl bends. [c] Full values of computed bending frequencies for reactant ion. [d] Transition-state frequencies taken as the product benzyne frequencies plus two C–Cl bends.

Table 4. CID Threshold Energies for Halophenyl Anions, Halobenzene Acidities, and Derived Heats of Formation for *ortho*-, *meta*-, and *para*-Benzyne[a]

halophenyl anion	E_T, n (eq 3)	ΔH_{acid}-(C_6H_5X)	$\Delta H^{\circ}_{f,298}$-(C_6H_4)[b]
ortho-Cl	16.1 ± 2.2, 1.59 ± 0.07	388.2 ± 2.0[c]	107 ± 3
meta-Cl	26.3 ± 2.0, 1.62 ± 0.09	390.2 ± 2.0[c]	119 ± 3
para-Cl	35.3 ± 2.0, 1.63 ± 0.05	389.7 ± 2.0[c]	127 ± 3
ortho-Br	9.2 ± 0.7, 1.65 ± 0.11	387 ± 3[d]	107 ± 4
meta-Br	16.1 ± 0.8, 1.64 ± 0.08	390 ± 3[d]	117 ± 4
para-Br	28.1 ± 1.6, 1.64 ± 0.06	390 ± 3[d]	129 ± 4
	Perdeuterated Reactant Ions		
ortho-Cl-d_4	16.1 ± 1.0, 1.60 ± 0.10	388.2 ± 2.0[c]	106.6 ± 3.0
meta-Cl-d_4	29.1 ± 1.7,[e] 1.52 ± 0.06	391.1 ± 2.0[f]	122.0 ± 3.1
para-Cl-d_4	41.4 ± 0.6,[e] 1.59 ± 0.02	393.9 ± 2.0[f]	137.3 ± 3.3

[a] All values in kcal/mol. [b] Equation 4. [c] Determined from anion proton affinity bracketing. [d] Estimated from chlorobenzene data. [e] Threshold energies corrected to zero-contamination by *ortho* isomer. [f] Determined by silane cleavage methods using undeuterated chlorophenyltrimethylsilanes.

chlorophenyl anion become essentially the same as those of *para*-benzyne (within ±10%) after only 50% elongation of the C–Cl bond from its equilibrium value of 1.75 Å. Given that this bond will probably be stretched by 2–3 times its equilibrium length at the dissociation transition state,[53] we conclude that the ν_{prod} model is more physically realistic. Finally, note that in order to have the contribution of the ion internal energy to the net shift in E_T exactly cancel the contribution of the kinetic shift, as would be required for the simple model in eq 2 to be valid, the reaction must have $\Delta S^{\ddagger}_{1000} \approx 14$ eu. However, this value is likely to be too high, considering that the analogous ionic dissociations involving cleavage of aryl–halogen atom bonds that have been previously characterized by time-resolved techniques have suggested activation entropies far less than this (2–8 eu).[39,52,53]

We conclude from the above analysis that the halophenyl anion CID data are best modeled by explicitly including the ion lifetime and internal energy effects. For the final analyses using eq 3, we shall adopt a relatively loose, "product-like" transition state model in which two bending frequencies of 25 cm^{-1} are added to the computed frequencies for the corresponding neutral benzyne product. For the undeuterated chlorophenyl anions, this corresponds to $\Delta S^{\ddagger}_{1000} = 6.2$–$7.7$ eu, and for bromophenyl anions this gives $\Delta S^{\ddagger}_{1000} = 7.0$–$8.0$ eu. Table 4 lists the derived threshold energies for CID of each isomeric chlorophenyl and bromophenyl anion. The indicated uncertainty in these values is determined by the precision in the measurements, the estimated uncertainty in the modeling procedure (0.05 eV[55]), and the uncertainty in the ion beam energy scale (0.15-eV lab frame = 0.04-eV CM frame).

Two additional factors that can affect appearance energy measurements need to be considered: "competitive shifts" due to fast competing reactions and reverse activation energies. The former effect can arise if electron detachment from the collisionally activated halophenyl anions (or some other reaction) occurs to such an extent that the cross sections for halide loss are suppressed. CID of fluorophenyl anions represents a probable case in point, since the electron binding energies of these anions are significantly less than their F^- binding energies, and anomalously high dissociation onsets and low CID yields are observed. The electron binding energies of chloro- and bromophenyl anions are not known experimentally, but they can be reasonably estimated to be in the range 1.4–1.6 eV (32–37 kcal/mol) from the gas-phase acidities of chloro- and bromobenzene and assumed C–H bond strengths of 111 kcal/mol (i.e., the same as in benzene). Thus, the energy requirement for electron detachment is greater than the apparent CID thresholds for all but *para*-chlorophenyl anion, where the two decomposition channels have similar energies. We can therefore conclude that electron detachment cannot be competitive with halide loss at threshold for most of the halophenyl anions. Moreover, because collision-induced electron detachment is believed to be inefficient at threshold,[56] it is unlikely to have any influence on the *para*-chlorophenyl anion results as well.

The measured CID thresholds strictly correspond to activation energies for dissociation. These will be useful for deriving thermochemical data only if they can be equated with the true bond energies, i.e., only if the reverse reactions, addition of a halide ion to *ortho*-, *meta*-, and *para*-benzyne, have negligible activation energies. Several lines of reasoning suggest that this is so. First of all, *ab initio* calculations, carried out in this laboratory[19] and others,[18,20,21] indicate that all three benzynes possess planar $\sigma^1\sigma^1$ singlet ground states. Therefore, halide dissociation from the necessarily singlet-state halophenyl anions can occur on a single diabatic potential energy surface (that is, it is both spin- and symmetry-allowed). Gas-phase nucleophilic additions to closed-shell unsaturated species such as carbonyl compounds, when exothermic, typically occur without barriers. Moreover, for anionic nucleophiles, the long-range electrostatic attractive forces between the ion and substrate will diminish or remove altogether any entrance-channel barriers that might otherwise exist. Therefore, the measured activation energies for halide loss are taken to be good estimates of the corresponding thermochemical bond dissociation energies.

A Discrepancy with Theory; Revised Measurements. Listed in Table 4 are the measured CID thresholds for the chloro- and bromophenyl anions analyzed with use of eq 3, along with the bracketed (or estimated) positional acidities for chlorobenzene and bromobenzene. The heats of formation for the benzynes derived from these data and the auxiliary data in Table 1 using eq 4 are listed in the last column. From the chlorophenyl anion data, the final heats of formation for **1**, **2**, and **3** are calculated to be 107 ± 3, 119 ± 3, and 127 ± 3 kcal/mol, respectively, where the uncertainties are the root-square-sum of the component uncertainties. From the bromophenyl anion results, the heats of formation for **1**, **2**, and **3** are determined to be 107 ± 4, 117 ± 4, and 129 ± 4 kcal/mol, respectively, in excellent agreement with the values obtained from the chlorophenyl anion precursors. The greater uncertainties in these latter values reflect the greater uncertainties in the estimated acidities.

Although the results obtained from the two different precursors are in excellent agreement, the heats of formation for *meta*- and *para*-benzyne are suspect since, as noted in the Introduction,

(55) For the chlorophenyl anions, this corresponds to an uncertainty in the dissociation activation entropy of at least ±2 eu.

(56) (a) Simons, J. *J. Am. Chem. Soc.* **1981**, *103*, 3971. (b) Foster, R. F.; Tumas, W.; Brauman, J. I. *J. Chem. Phys.* **1983**, *79*, 4644.

Scheme 3

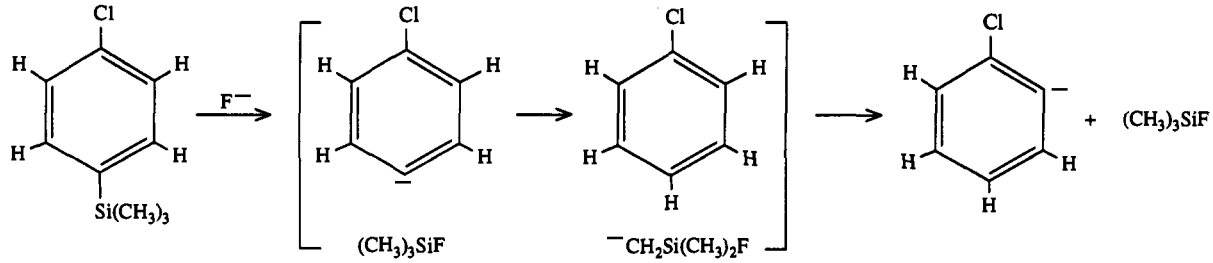

high-level *ab initio* molecular orbital calculations predicted significantly higher values.[19-21] Multiconfigurational SCF and CI calculations of the energy changes associated with the hypothetical isodesmic reaction 6 for each singlet-state benzyne

$$C_6H_4(\mathbf{1}, \mathbf{2}, \text{or } \mathbf{3}) + C_6H_6 \rightarrow 2C_6H_5 \qquad (6)$$

when combined with the known heats of formation for benzene and an updated value for phenyl radical (Table 1) give predicted heats of formation for **1**, **2**, and **3** of 104.8, 122.3, and 136.2 kcal/mol, respectively, with estimated accuracies of ±3.0 kcal/mol.[19] The credibility of these calculations, as evidenced by the excellent correspondence with experiment on the absolute heat of formation and singlet–triplet splitting in *ortho*-benzyne (ΔE_{ST}(theory) = 36.9 kcal/mol;[19] ΔE_{ST}(exptl) = 37.7 ± 0.6 kcal/mol),[57] convinced us that the experimental heats of formation for *meta*- and *para*-benzyne must be in error, despite the internal consistency of the two independent sets of measurements.

In seeking an explanation for the apparent failure of the CID threshold measurements for **2** and **3**, we first considered the possibilities for formation of lower energy products in the CID reactions. For *para*-benzyne, ring-opening during CID could conceivably produce *cis*-3-hexene-1,5-diyne (**4**) by a retro-Bergman cyclization (eq 7). Using Benson group equivalents,[58]

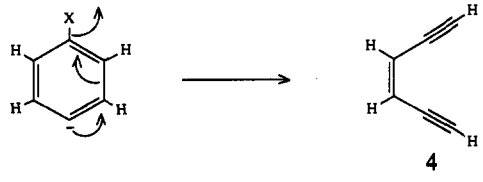

(7)

the heat of formation of **4** is calculated to be 124 kcal/mol, a value that is comparable to the measured value for **3**. However, Jones and Bergman[5] measured the activation energy for ring-closure of **4** to be 32 kcal/mol. If we assume for the moment that the theoretical value for ΔH_f(**3**) (136 kcal/mol) is correct, then the calculated activation energy for ring-opening of *para*-benzyne is 32 − (136 − 124) = 20 kcal/mol. If ring-opening to produce **4** occurred during decomposition of a *para*-halophenyl anion, then the measured CID threshold would necessarily reflect some or all of this activation energy, and an apparent heat of formation for **3** as high as 136 + 20 = 156 kcal/mol would be obtained. That the measured heat of formation obtained *from two different halophenyl anion precursors* is considerably less than 156 kcal/mol makes this explanation highly unlikely. Moreover, since there are no low-energy ring-opening pathways available at all to *meta*-halophenyl anions, formation of acyclic C_6H_4 products can be safely ruled out.

Formation of the bicyclic hydrocarbon isomers bicyclo[3.1.0]-hexa-1,3,5-triene and bicyclo[2.2.0]hexa-1,3,5-triene can also be ruled out, since reliable *ab initio* MO calculations[19,20] locate these species 11 and 51 kcal/mol higher in energy than **2** and **3**, respectively.

A clue as to the origins of the apparently low heats of formation can be found in Figure 2. If deliberate addition of water to the flow tube can cause such a dramatic shift in the *meta*- and *para*-halophenyl anion appearance curves, then what would be the effect of traces of adventitious water (or other Brønsted acids) that are all but unavoidable in the instrument? Because of the much larger CID cross section for *ortho*-chlorophenyl anion compared to *meta*- and *para*-chlorophenyl anions, the presence of even a small amount of *ortho* isomer as a contaminant could have a significant effect on the derived thresholds for the *meta* and *para* isomers. We have modeled this effect in the following manner. The theoretically predicted heat of formation for **3**,[19] when combined with the bracketed *para*-position acidity of chlorobenzene according to eq 4, leads to an estimate for the CID threshold for *para*-chlorophenyl anion of about 44 kcal/mol (1.9 eV). Deconvolution of variably scaled cross sections for a representative *ortho*-chlorophenyl anion appearance curve from a representative *para*-chlorophenyl anion data set shows that only *ca.* 2% *ortho* contamination is necessary to shift the derived threshold from the theoretical value at 1.9 eV to the measured value of 1.5 eV! Similarly, only 13% *ortho* impurity in the *meta*-chlorophenyl anion experiment is required to produce the apparent 5 kcal/mol lowering of the CID threshold compared to the theoretically predicted value. The greater amount of impurity required for the *meta* isomer arises from its larger CID cross section and the smaller difference between the two thresholds.

It is clear from this exercise that the *meta*- and *para*-halophenyl anions must be completely free of *ortho*-halophenyl anion contamination in order to obtain the correct CID thresholds and that this sort of contamination problem was probably the origin of the low thresholds and correspondingly low heats of formation for **2** and **3** obtained earlier.[17] Although achieving a scrupulously dry flow reactor is not an impossiblity, it may not completely solve the problem anyway, since the nascent $(CH_3)_3SiF$ product of the fluoride-induced desilylation reactions used to form *meta*- and *para*-halophenyl anions could also conceivably catalyze the isomerization prior to dissociation of the ion/molecule complex, as illustrated in Scheme 3.

A better solution involves the use of ring-deuterated precursors. For example, reaction of F^- with *para*-(chlorophenyl)trimethylsilane-d_4 produces the completely deuterated *para*-chlorophenyl anion with m/z 115 (for the all-$^{35}Cl^{12}C$ isotopomer). Acid-catalyzed rearrangement of this ion, either by adventitious water (Scheme 2) or by the departing $(CH_3)_3SiF$ group during fluoride-induced desilylation (Scheme 3), would necessarily replace a deuterium with a hydrogen, thereby changing the mass of the ion to m/z 114.[59] Therefore, by mass-selecting only the chlorophenyl-d_4 anion isotopomer with m/z 115 for the CID threshold measurements, rearranged ions can be excluded and the reactant ion beam should be nearly "pure" (*vide infra*). The needed chlorotrimethyl-d_4-silanes were synthesized and used as chlorophenyl-d_4 anion precursors to test this strategy. The normalized

(57) Leopold, D. G.; Miller, A. E. S.; Lineberger, W. C. *J. Am. Chem. Soc.* **1986**, *108*, 1379.

(58) (a) Benson, S. W. *Thermochemical Kinetics*; Wiley & Sons: New York, 1976. (b) Benson, S. W.; Garland, L. J. *J. Phys. Chem.* **1991**, *95*, 4915.

(59) Catalysis by the neutral *para*-(chlorophenyl)trimethylsilane is also a possibility that might not be distinguished by the labeling experiments described here. However, it has been found that the thresholds are essentially independent of neutral precursor flow rate, indicating that this is not a significant problem. Nevertheless, the experiments were carried out using as low a neutral precursor flow rate as possible to minimize the possibility of catalyzed isomerization.

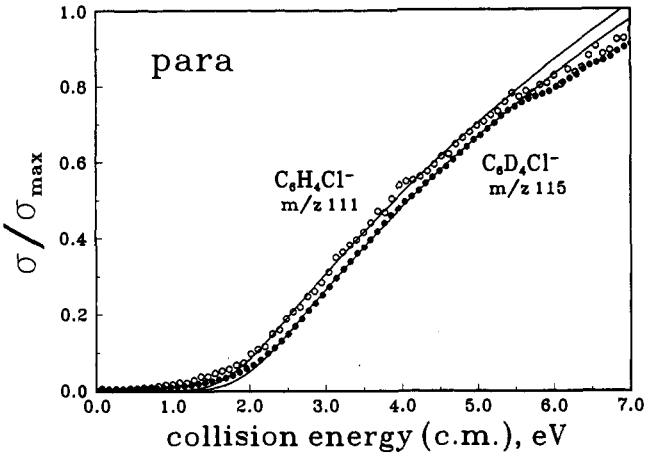

Figure 4. Relative cross sections for collision-induced dissociation of Cl^- from deuterated (solid circles) and undeuterated (open circles) *para*-chlorophenyl anions as a function of translational energy in the center-of-mass frame. The solid lines are the model appearance curves calculated using eq 3 and the transition-state model discussed in the text.

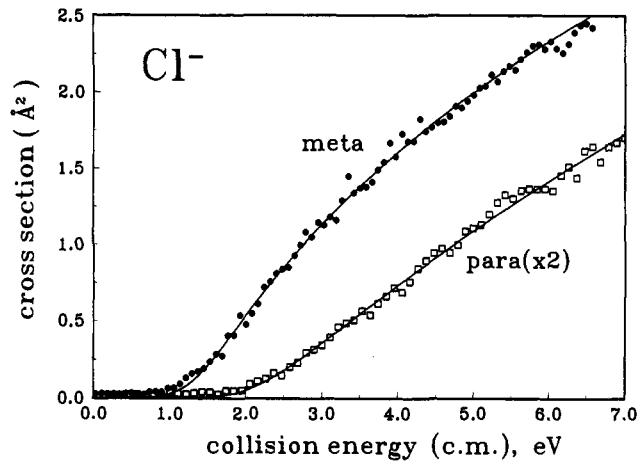

Figure 5. Cross sections for collision-induced dissociation of Cl^- from *meta*- and *para*-chlorophenyl-d_4 anions extrapolated to 0% *ortho* isomer contamination. See text for discussion of extrapolation procedure.

cross section for Cl^- elimination from deuterated *para*-chlorophenyl anions is shown in Figure 4, along with the measured Cl^- appearance curve obtained under similar conditions from the corresponding undeuterated ion. The predicted shift in the dissociation onset is clearly evident. Moreover, the discernible low-energy "tail" in the undeuterated *para*-chlorophenyl anion data is much less pronounced in the data for the corresponding deuterated ion (cf. Figure 1), providing further evidence for the removal of *ortho* isomer contamination. That the difference in behavior between the deuterated and undeuterated ions is not due to secondary deuterium isotope effects on the dissociation energies is shown by the fact that the appearance curves obtained for *ortho*-chlorophenyl-d_4 and -d_0 anions are indistinguishable.

Although the appearance curves obtained from CID of the perdeuterated chlorophenyl anions display the anticipated shifts relative to the undeuterated ions, simply choosing the chlorophenyl-d_4 anions for CID threshold analysis is still insufficient for completely removing the *ortho*-chlorophenyl isomer contamination. This is because, in each of the chlorophenyl-d_4 anion experiments, significant amounts (≥30%) of the corresponding d_3 species are present, presumably due to H/D exchange of the d_4 ions and formation of *ortho*-chlorophenyl isomers (cf. Schemes 2 and 3). Although the nominal mass of the major d_3 isotopomer ($^{35}Cl^{12}C_6D_3H$) is m/z 114, and therefore not an interference, the [M + 1] isotopomer due to natural abundance ^{13}C has m/z 115. Since this will amount to approximately 6.7% of the main d_3 isotopomer signal intensity, significant amounts of impurity can be present in the mass-selected m/z 115 ion beam.

Therefore, in order to obtain the true CID thresholds for completely pure *meta*- and *para*-chlorophenyl anions, it is necessary to measure the cross sections as a function of the corresponding d_3-[M + 1] signal intensities and then extrapolate to zero contamination. In practice, this was accomplished by deliberate addition of varying amounts of water to the flow tube in which a deuterated chlorophenyl anion had been prepared. The (m/z 114)/(m/z 115) signal intensity was determined, followed by measurement of the cross section for $^{35}Cl^-$ loss resulting from CID of the mass-selected ions with m/z 115. The fraction of the m/z 115 ion that is d_3-[M + 1] impurity is given by the relation percent d_3-[M + 1] = $[I_{114}/I_{115}] \times 6.7$. In the case of the *meta*-chlorophenyl anion, 14 data sets were used with the percent d_3-[M + 1] values ranging from 1.6 to 9.1%. For *para*-chlorophenyl anion, 12 data sets were used with 2.2–6.5% d_3-[M + 1]. The cross sections measured as a function of percent d_3-[M + 1] impurity were then linearly extrapolated to zero contamination, and the thresholds for the extrapolated cross sections were obtained by the use of eq 3 as described earlier. The zero-contamination cross sections and the corresponding fits are shown in Figure 5. The thresholds obtained from these curves using eq 3 are 1.24 and 1.79 eV for *meta*- and *para*-chlorophenyl anions, respectively. Analogous "zero-contaminant" extrapolation experiments with bromophenyl-d_4 anions could not be performed. This is due to the extensive signal loss described earlier that occurs with bromophenyl anions in the presence of water or other potential acid catalysts. For this reason, it was not possible to vary the ratio of bromophenyl-d_3 anions/bromophenyl-d_4 anions to a significant extent while maintaining sufficient signal intensity for reliable CID threshold measurements.

The final CID threshold energy determined for the *ortho*-chlorophenyl-d_4 anion and those obtained from the extrapolated cross sections for *meta*- and *para*-chlorophenyl-d_4 anions are listed in the bottom section of Table 4, along with the average n value from the analyses using eq 3. The indicated uncertainties are computed from the square-root of the sum-of-squares of the component uncertainties. This includes the precision of the threshold measurements (taken as the standard deviations of the measured thresholds for the undeuterated chlorophenyl anions: 0.06 eV), the uncertainty introduced by the cross section extrapolations for the *meta*- and *para*-chlorophenyl anions (conservatively estimated by the difference in the threshold energies obtained from extrapolated cross sections obtained on two different days: 0.05 eV for *meta* and 0.07 eV for *para*), the uncertainty in the transition state model used for the threshold analysis (0.05 eV[55]), and the uncertainty in the ion beam energy scale (0.04 eV).

The final CID thresholds measured for the deuterated and undeuterated *ortho*-chlorophenyl anions are identical (Table 4). This validates the reasonable expectation that the secondary deuterium isotope effect on the chloride dissociation reaction is negligible. Therefore, the dissociation energies determined from the perdeuterated chlorophenyl anions can be used directly with eq 4 to determine the heats of formation for the undeuterated benzynes.

Recognizing the relative ease with which acid-catalyzed isomerization of *meta*- and *para*-halophenyl anions to the *ortho* isomer apparently takes place led us to question the reliability of the bracketed proton affinities of *meta*- and *para*-chlorophenyl anions. It is not difficult to imagine a scenario wherein bracketing experiments would give erroneous results (ΔH_{acid} too low) if the added reference acids can isomerize the more strongly basic *meta*- and *para*-chlorophenyl anions to the less basic *ortho* isomer. For this reason, we redetermined the *meta* and *para* position acidities for chlorobenzene using an alternative experimental procedure. The method used represents a minor variation on the silane cleavage technique developed by DePuy and co-workers[60] and

Scheme 4

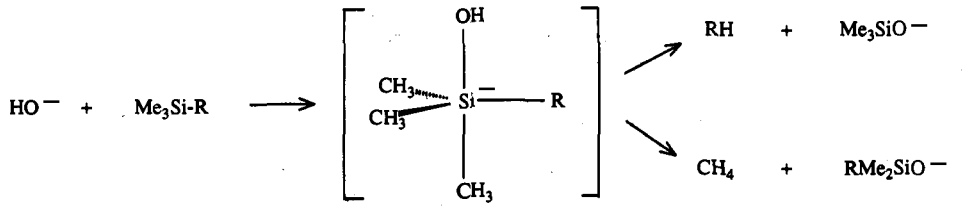

used by others[61] to determine the acidities of alkanes. Full details for these acidity measurements will be published elsewhere,[62] and only a brief summary is provided here. The procedure involves determination of the relative yields of trialkylsiloxide ion products that result from the reaction of HO^- with alkyltrimethylsilanes (Scheme 4). The relative amount of the two siloxide ions formed in these reactions has been shown to be a sensitive function of the acidity difference between methane and the other neutral fragment, RH.[60,61] The statistically corrected ratio for (RH loss)/(CH_4 loss), given by $R = 3[Me_3SiO^-]/[RMe_2SiO^-]$, is related to the difference in gas-phase acidity between RH and CH_4 according to eq 8a. The value of β was determined by calibration

$$\ln(R) = -\beta[\Delta H_{acid}(RH) - \Delta H_{acid}(CH_4)] \quad (8a)$$

$$\ln(R') = -\beta'[\Delta H_{acid}(RH) - \Delta H_{acid}(PhH)] \quad (8b)$$

using the known acidities of methane,[47] dimethyl ether,[60] benzene,[41] and propene[47] and is found to be 0.118 mol/kcal (r^2 = 1.00). Using this value for β along with the measured siloxide ratios from reactions of HO^- with *meta*- and *para*-(chlorophenyl)-trimethylsilane, the gas-phase acidities of the *meta* and *para* positions of chlorobenzene are found to be 391.1 and 394.0 kcal/mol, respectively.

In order to obtain an independent check on these results, silanes of the form $SiMe_2(Ph)R$ were also examined. For these systems the ratio of RH loss versus PhH loss from reaction with HO^- must be determined and calibrated with known RH acidities. The relationship between the measured product ion signal ratio, $R' = [PhMe_2SiO^-]/[RMe_2SiO^-]$, and the difference in acidities is shown in eq 8b. Using allylphenyldimethylsilane as a calibrant, the value of β' was found to be 0.124 mol/kcal. Determination of the siloxide ion yield ratios for the appropriate silanes and use of eq 8b give *meta* and *para* acidities for chlorobenzene of 391.0 and 393.8 kcal/mol, respectively, in good agreement with the values derived above. The final acidities taken as the average of the two sets of measurements are listed in the bottom section of Table 4. Additional support for the revised acidities for the chlorobenzene system comes from *ab initio* molecular orbital calculations. At the MP4SDTQ/6-31+G*//4-31G + ZPE level,[63] the *ortho* position of chlorobenzene is calculated to be 2.9 kcal/mol more acidic than the *meta* position, and 5.1 kcal/mol more acidic than the *para* position, in good agreement with the experimental differences determined from the silane cleavage reactions. While the redetermined acidity for the *meta* position of chlorobenzene is close to the values obtained from the bracketing experiments, the revised acidity for the *para* position differs by *ca.* 4 kcal/mol from the bracketed values. This provides a clear illustration of the inherent problems associated with the use of bracketing procedures to determine the basicity of the higher energy tautomeric form of an anion.

The 298 K heats of formation derived for the three benzynes from the revised measurements and the auxiliary data in Table 1 are listed in the last column of Table 4; for **1**, **2**, and **3** they are 106.6 ± 3.0, 122.0 ± 3.1, and 137.3 ± 3.3 kcal/mol, respectively, where the assigned uncertainty is the square-root of the sum-of-squares of the component uncertainties.

Derived Thermochemical Properties. The measured heats of formation for **1**, **2**, and **3** can be used to derive other useful thermochemical data. For example, Gronert and DePuy[45] recently examined the gas-phase reactions of the dehydrophenyl anion **5** (eq 9), which was prepared by CID of deprotonated

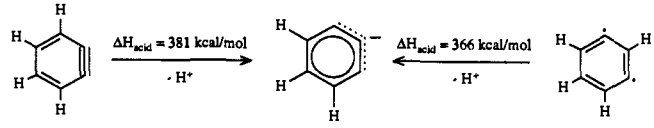

1 5 2

fluorobenzene. By bracketing the proton affinity of this ion, they estimated ΔH_{acid}(*ortho*-benzyne) to be 381 kcal/mol. Using ΔH_f(**1**) = 106.6 ± 3.0 kcal/mol from the present work, the heat of formation of **5** is calculated to be 122 ± 3 kcal/mol. Dehydrophenyl anion **5** is also produced by the hypothetical deprotonation of *meta*-benzyne (**2**) in the 2-position (eq 9). Using ΔH_f(**2**) from this study, the gas-phase acidity of *meta*-benzyne in this position is calculated to be 366 kcal/mol, a value which is 34 kcal/mol lower than that for benzene.

The absolute heats of formation of the benzynes allow a determination of the *second* C–H bond strengths in benzene, i.e., the *ortho*, *meta*, and *para* C–H bond strengths in phenyl radical. The first C–H bond energy in benzene has been subject to some controversy. The value $D_{298}[C_6H_5\text{-}H]$ = 110.9 ± 2.0 kcal/mol originally recommended by McMillen and Golden[64] was recently adjusted to 113.5 ± 2.6 kcal/mol by Tsang.[65] In a recent review, Berkowitz, Ellison, and Gutmann[66] recommend a value of 111.2 ± 0.8 kcal/mol based on the thermochemical relationship $DH_{298}[C_6H_5\text{-}H] = \Delta H_{acid}(C_6H_6) + EA(C_6H_5) - IP(H) + T_{corr}$, where T_{corr} is the difference in 0–298 K integrated heat capacities of phenyl anion and phenyl radical. The gas-phase acidity of benzene, $\Delta H_{acid}(C_6H_6)$, has been determined at 600 K by proton-transfer equilibrium methods in a high-pressure mass spectrometer to be 400.7 ± 0.6 kcal/mol[41] and corresponds to ΔH_{acid} at 298 K of 399.8 ± 0.8 kcal/mol. The electron affinity of phenyl radical, $EA(C_6H_5)$, was recently determined from negative ion photoelectron measurements to be 1.096 ± 0.006 eV (25.3 ± 0.1 kcal/mol).[67] From these data and the well-known value for IP(H) = 313.6 kcal/mol, the above equation gives $DH_{298}[C_6H_5\text{-}H]$ = 111.2 ± 0.8 kcal/mol. This bond enthalpy corresponds to a 298 K heat of formation for the phenyl radical of 78.8 ± 0.8 kcal/mol. Combining this with the measured heats of formation for **1**, **2**, and **3** in a simple thermochemical cycle gives *ortho*, *meta*, and *para* C–H bond strengths in phenyl radical of 79.9 ± 3.1, 95.3

(60) (a) DePuy, C. H.; Bierbaum, V. M.; Damrauer, R. *J. Am. Chem. Soc.* **1984**, *106*, 4051. (b) DePuy, C. H.; Gronert, S.; Barlow, S. E.; Bierbaum, V. M.; Damrauer, R. *J. Am. Chem. Soc.* **1989**, *111*, 1968.

(61) Peerboom, R. A. L.; Rademaker, G. J.; de Konig, L. J.; Nibbering, N. M. M. *Rapid Commun. Mass Spectrom.* **1992**, *6*, 394.

(62) Wenthold, P. G.; Squires, R. R. Manuscript in preparation.

(63) Frisch, M. J.; Head-Gordon, M.; Trucks, G. W.; Foresman, J. B.; Schlegel, H. B.; Raghavachari, K.; Robb, M. A.; Binkley, J. S.; Gonzales, C.; Defrees, D. J.; Fox, D. J.; Whiteside, R. A.; Seeger, R.; Melius, C. F.; Baker, J.; Martin, R. L.; Kahn, L. R.; Stewart, J. J. P.; Topiol, S.; Pople, J. A. *Gaussian 90*; Gaussian, Inc.: Pittsburgh, PA, 1990.

(64) McMillen, D. F.; Golden, D. M. *Ann. Rev. Phys. Chem.* **1982**, *33*, 493.

(65) Robaugh, D.; Tsang, W. *J. Phys. Chem.* **1986**, *90*, 5363.

(66) Berkowitz, J.; Ellison, G. B.; Gutman, D. *J. Phys. Chem.* **1994**, *98*, 2744. We thank Professor Ellison for a copy of this review in advance of publication.

(67) Gunion, R.; Gilles, M.; Polak, M.; Lineberger, W. C. *Int. J. Mass Spectrom. Ion Processes* **1992**, *117*, 601.

± 3.2, and 110.6 ± 3.4 kcal/mol, respectively. The marked reduction in the bond strengths in the *ortho* and *meta* positions is largely, although not entirely, a reflection of the singlet stabilization in the corresponding biradicals due to direct overlap of the σ orbitals at the dehydro carbons. These effects are described in detail in our recent theoretical investigation.[19]

Finally, we can use the measured heat of formation for **3** along with the estimated heat of formation for *cis*-3-hexene-1,5-diyne (**4**) of 124 ± 2[58] to determine that the Bergman cyclization reaction is endothermic by 13 kcal/mol (eq 10a). It is noteworthy in this regard that cyclization of **4** is known to have a substantial activation energy (32 kcal/mol) and is reported to occur with extremely low efficiency under pyrolytic conditions.[68] In contrast, the closely related cycloaromatization reaction of *cis*-1,2,4-heptatrien-6-yne to α,3-dehydrotoluene (eq 10b) is exothermic by 15 kcal/mol[69] and occurs rapidly even at reduced temperatures.[6]

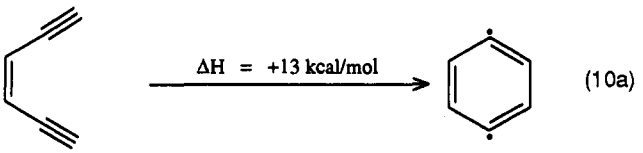

(10a)

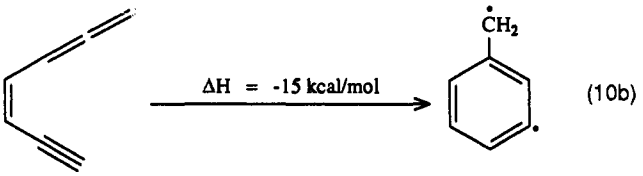

(10b)

Concluding Remarks. In addition to the specific thermochemical conclusions derived from this work that are reiterated below, several important general conclusions can be made about the experimental methods we have employed. First of all, it is clear from this work that CID threshold measurements for α,ω-elimination reactions can be *extremely* sensitive to small amounts (1–2%) of isomeric impurities in the reactant ion beam if this contaminant yields the same CID fragment ion with a greater efficiency and lower threshold energy than the main component. This will always be a danger with any type of haloaryl anion or with any other system in which higher energy isomers of the reactant ion can be easily converted to a lower energy, more labile form. This problem can be overcome, to a large extent, by strategic use of deuterated precursors for the desired reactant, since mass-selection of the perdeuterated ion can almost completely remove the isomeric impurity from the beam. Nevertheless, some contamination may still remain as an isobaric species with the isomerized structure. In this case, extrapolation to the contaminant-free threshold energy can be performed to arrive at the true value.

Second, use of bracketing procedures for obtaining the proton affinity of an anion can lead to erroneous (too low) results if the anion easily converts to a lower energy (weaker base) isomer by acid–base catalysis. The DePuy silane cleavage technique can provide a useful and accurate alternative method for determining absolute heats of formation for aromatic halocarbanions.[62]

Finally, a systematic evaluation of the influence of reactant ion internal energy and dissociation lifetimes on the derived CID thresholds reveals small, but non-negligible effects. For the halophenyl anions examined in this study and, presumably, for other related systems, the dissociation transition states are best treated as relatively loose, product-like species with the two bending frequencies associated with the dissociating carbon–halide bond both near 25 cm^{-1} and with activation entropies ($\Delta S^{\ddagger}_{1000}$) in the 3–8-eu range.

The revised thermochemical measurements yield final values for the absolute heats of formation of the benzynes that are in excellent agreement with the theoretically predicted values; the final experimental values are $\Delta H^{\circ}_{f,298}$(**1**) = 106.6 ± 3.0 kcal/mol, $\Delta H^{\circ}_{f,298}$(**2**) = 122.0 ± 3.1 kcal/mol, and $\Delta H^{\circ}_{f,298}$(**3**) = 137.3 ± 3.3 kcal/mol. From these data, values for the *ortho*, *meta*, and *para* bond strengths in phenyl radical are determined to be 79.9 ± 3.1, 95.3 ± 3.2, and 110.6 ± 3.4 kcal/mol, respectively. The differences between these values and the first C–H bond strength in benzene (111.2 ± 0.8 kcal/mol) give rough approximations for the singlet–triplet splittings in the corresponding ground-state singlet *ortho*-, *meta*-, and *para*-benzynes of 31, 16, and 1 kcal/mol, respectively.[70] *meta*-Benzyne (**2**) is predicted to be an unusually strong C–H acid (ΔH_{acid}(2-position) = 366 ± 3 kcal/mol), a fact that may aid in its eventual detection in the gas phase. The Bergman reaction, i.e., cyclization of *cis*-3-hexene-1,5-diyne (**4**) to *para*-benzyne (eq 10a), is determined to be endothermic by 13 ± 3 kcal/mol.

We are currently extending what we have learned in this investigation about CID threshold measurements for α,ω-elimination reactions to a variety of other σ,σ-biradicals such as the dehydronaphthalenes and α,n-dehydroindenes, σ,π-biradicals such as the α,n-dehydrotoluenes and phenols, and π,π-biradical systems such as the xylylenes. The results of these ongoing studies will be presented in future publications from this laboratory.

Acknowledgment. We are grateful to Dr. Lee Sunderlin for his help with the CID threshold analyses, Capt. Scott Wierschke for calculations on chlorophenyl anions, and Prof. Wes Borden, Dr. Athanassios Nicolaides, and Prof. Dieter Cremer for sharing their computational results for the benzynes in advance of publication. This work was supported by the National Science Foundation and the Department of Energy, Office of Basic Energy Science. P.G.W. thanks the Department of Education and Phillips Petroleum for a fellowship.

(68) Chen, P. Private communication.

(69) (a) Wenthold, P. G.; Wierschke, S. G.; Nash, J. J.; Squires, R. R. *J. Am. Chem. Soc.* **1993**, *115*, 12611. (b) Wenthold, P. G.; Wierschke, S. G.; Nash, J. J.; Squires, R. R. *J. Am. Chem. Soc.*, in press.

(70) Zhang, X.; Chen, P. *J. Am. Chem. Soc.* **1992**, *114*, 3147.